Journal of Alloys and Compounds 504 (2010) 217–223

Contents lists available at ScienceDirect

Journal of Alloys and Compounds

journal homepage: www.elsevier.com/locate/jallcom

Growth, structural, Raman, and photoluminescence properties of rutile TiO_2 nanowires synthesized by the simple thermal treatment

Hyoun Woo Kim[a,*], Hyo Sung Kim[a], Han Gil Na[a], Ju Chan Yang[a], Doo Young Kim[b]

[a] Division of Materials Science and Engineering, Inha University, Incheon 402-751, Republic of Korea
[b] Department of Chemistry, Michigan State University, East Lansing, MI 48824, USA

ARTICLE INFO

Article history:
Received 27 December 2009
Received in revised form 21 May 2010
Accepted 21 May 2010
Available online 8 June 2010

Keywords:
TiO_2
Nanowires
Raman
Photoluminescence
Thermal treatment

ABSTRACT

We have used the simple heating technique for growing TiO_2 nanowires. We have changed the thickness of predeposited Au layers on TiAlN substrates, realizing that the thickness of the Au layer influenced the resultant morphology of nanowires. The nanowires were analyzed with X-ray diffraction (XRD), scanning electron microscopy (SEM), transmission electron microscopy (TEM), Raman spectroscopy, and photoluminescence spectroscopy (PL). The resultant nanowires consisted of the tetragonal rutile structure of TiO_2. With the nanowire morphology changing with varying the Au layer thickness, we suggest that the associated growth mechanism is a base-growth mode, in which Au played a catalytic role. PL spectra indicated that the TiO_2 nanowires exhibited a broad emission band comprising four peaks centered at 3.0, 2.6, 2.3, and 1.5 eV.

1. Introduction

The one-dimensional (1D) TiO_2 nanostructures such as nanotubes and nanowires have a large surface area, with its unique 1D morphology providing a direct path for electron transport with enhanced carrier collection [1,2]. As a result, 1D nanomaterials of TiO_2 have gained great attention for promising applications in photocatalyst [3–5], environmental purification, solar cell [6], gas [7] or humidity [8–12] sensor, antireflection coating [13], high-k dielectrics [14], and optoelectronics [15]. In addition, owing to their sharp tips and high aspect ratio, i.e., high electric-field enhancement effect as well as stable physical and chemical properties, 1D nanomaterials of TiO_2 have demonstrated to have good field emission properties [16], thereby making the materials suitable for applications in field emission display, vacuum electron sources, and so on.

The properties of nanocrystalline TiO_2 would be further extended if morphologies, size, compositions, and texture of the material were modified and the formation mechanisms of TiO_2 with different shape remain a challenge to the scientist in this field. Up to the present, researchers have therefore focused on the production of nanostructured TiO_2 using different techniques such as metalorganic chemical vapor deposition (MOCVD) [17,18], treatment with NaOH aqueous solution [19], electrodeposition [20], and hydrolysis process [21,22].

In this communication, we report for the first time the production of TiO_2 nanowires, by the simple heating of Au-coated TiAlN substrates. Among the three polymorphs of TiO_2, i.e., anatase, rutile, and brookite, the rutile phase exhibits excellent physical and chemical properties that have made it most widely used in pigments and cosmetics [23]. Although TiO_2 nanowires have been easily fabricated in anatase phase, the preparation of rutile-phased TiO_2 nanowires was rarely investigated. For example, rutile-phased TiO_2 nanowires have been fabricated via a two-step thermal evaporation method using Ti powders [24].

2. Experimental

First, the Si wafer with the oxide layer was purchased from Hissan Co. Ltd., Seoul, Korea. The Si (1 0 0) wafer was cleaned in buffer oxide etchant (BOE) solution and subsequently thermally oxidized, in which dry oxidation technique has been employed. On top of this layer, a 200 nm layer of TiAlN was deposited using a DC magnetron sputtering machine with a Ti/Al target, in an Ar/N_2 atmosphere. For the deposition of TiAlN, we used a substrate temperature, a DC power, and a pressure of 25 °C, 3 kW, and 5 mTorr, respectively. The overall composition of the coatings was $Ti_{0.35}Al_{0.15}N_{0.50}$.

Secondly, we fabricated the Au-coated TiAlN substrates, in which we used Si as starting materials onto which a layer of Au was deposited by the sputtering. Since one of our objectives was to investigate the effect of Au-coated substrate with respect to its thickness, we have varied the Au layer thickness in the range of 3–27 nm.

The growth process was carried out in a quartz tube (diameter 55 mm) in a horizontal tube furnace, which has been described elsewhere [25]. On top of the alumina boat, a piece of the Au-coated TiAlN substrate was placed with the Au-

* Corresponding author.
E-mail address: hwkim@inha.ac.kr (H.W. Kim).

0925-8388/$ – see front matter © 2010 Elsevier B.V. All rights reserved.
doi:10.1016/j.jallcom.2010.05.094

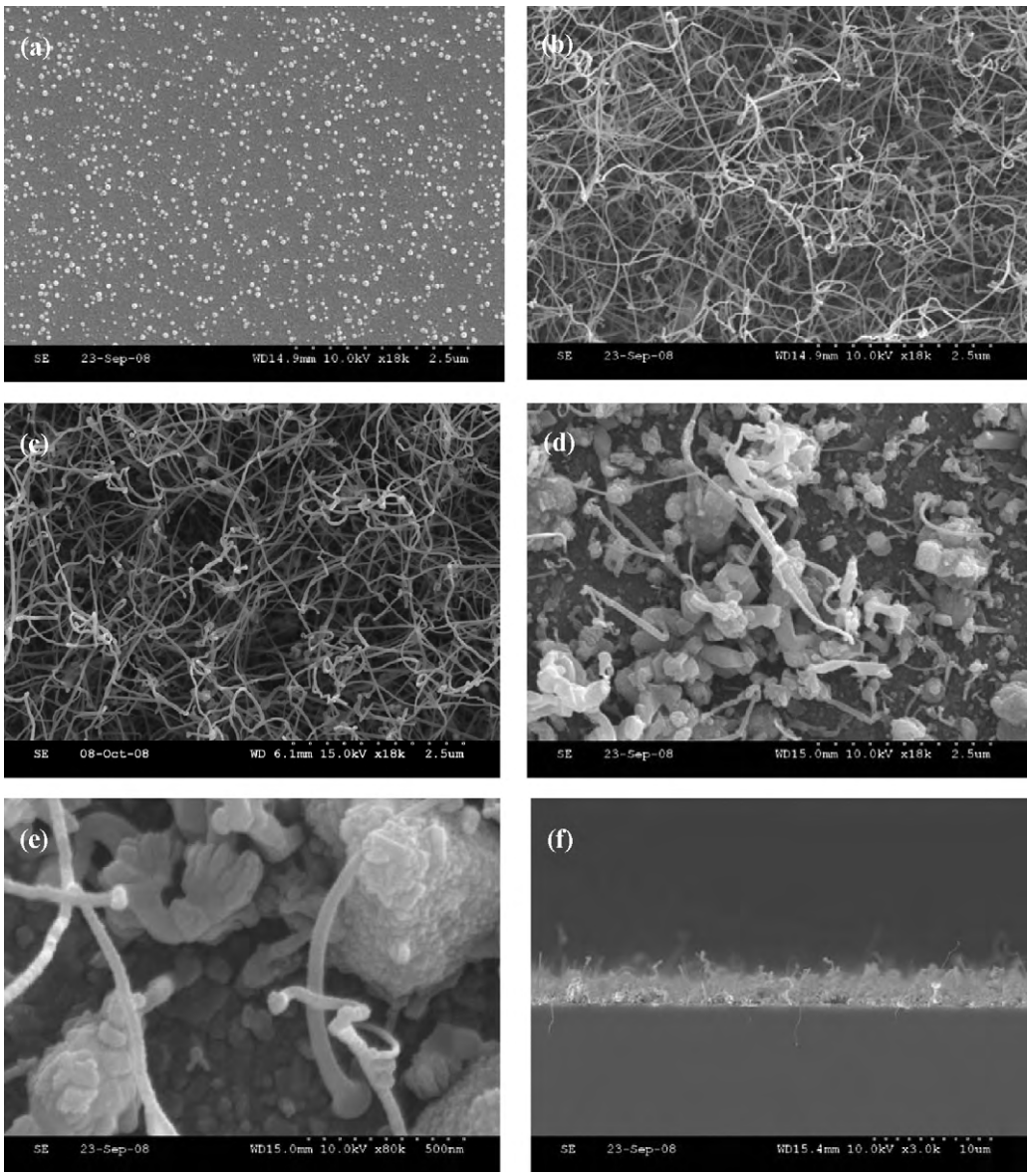

Fig. 1. Top-view SEM images of the products by heating (a) the uncoated TiAlN substrates and by heating the Au-coated TiAlN substrates with Au thicknesses of (b) 3, (c) 5, and (d) 9 nm. (e) The enlarged top-view image and (f) side-view image with respect to (d).

coated side downwards. The substrate temperature was set to 1050 °C for 2 h, with an air flow being maintained at 300 mTorr.

The samples were examined using glancing angle (0.5°) X-ray diffraction (XRD, X'pert MPD-Philips with $CuK\alpha_1$ radiation), scanning electron microscopy (SEM, Hitachi S-4200), and transmission electron microscopy (TEM, Philips CM-200) with energy-dispersive X-ray (EDX) spectroscopy attached. TEM samples can be prepared by sonicating the wire-grown substrate in acetone by ultrasonic treatment. A drop of the dispersion solution was then placed on a porous carbon film supported on a copper (Cu) microgrid. Micro-Raman spectra were taken on a Renishow Ramoscope equipped with a He–Ne laser ($\lambda = 633$ nm). PL measurements were performed at room temperature using a He–Cd laser with a wavelength of 325 nm as the excitation source (Kimon, 1K, Japan).

3. Results and discussion

We have examined the morphology and size of the resulting product by observing the SEM images. Fig. 1a shows a top-view SEM image of the product with uncoated TiAlN substrate, whereas Fig. 1b, c, and d shows those of the products grown by heating the Au-coated TiAlN substrate with a Au thickness of 3, 5, and 9 nm, respectively. Particle-like or cluster-like structures were observed on the uncoated substrate (Fig. 1a), whereas 1D nanowires were deposited on the Au-coated substrates (Fig. 1b–d). However, close examination of Fig. 1d indicates that the product with a Au thickness of 9 nm consists of wire and dots. Enlarged top-view image (Fig. 1e) and side-view image (Fig. 1f) reveal that the dots correspond to the clusters or particles. Furthermore, the clusters or particles were not a part of the wires. Instead, those clusters/particles have been directly grown from the substrate.

In order to estimate the average diameter of the nanowires, we have carried out a statistical analysis of SEM images. The diameter distributions of samples grown with the Au layer thickness of 3, 5, 9, and 27 nm, respectively, are shown in Fig. 2a, b, c, and d, in which the maxima of the diameter distributions occur in a range of 30–40, 40–50, 80–90, and 100–110 nm. Based on Fig. 2, we estimated that the average diameter of nanowires grown with the Au layer thickness of 3, 5, 9, and 27 nm, respectively, were about

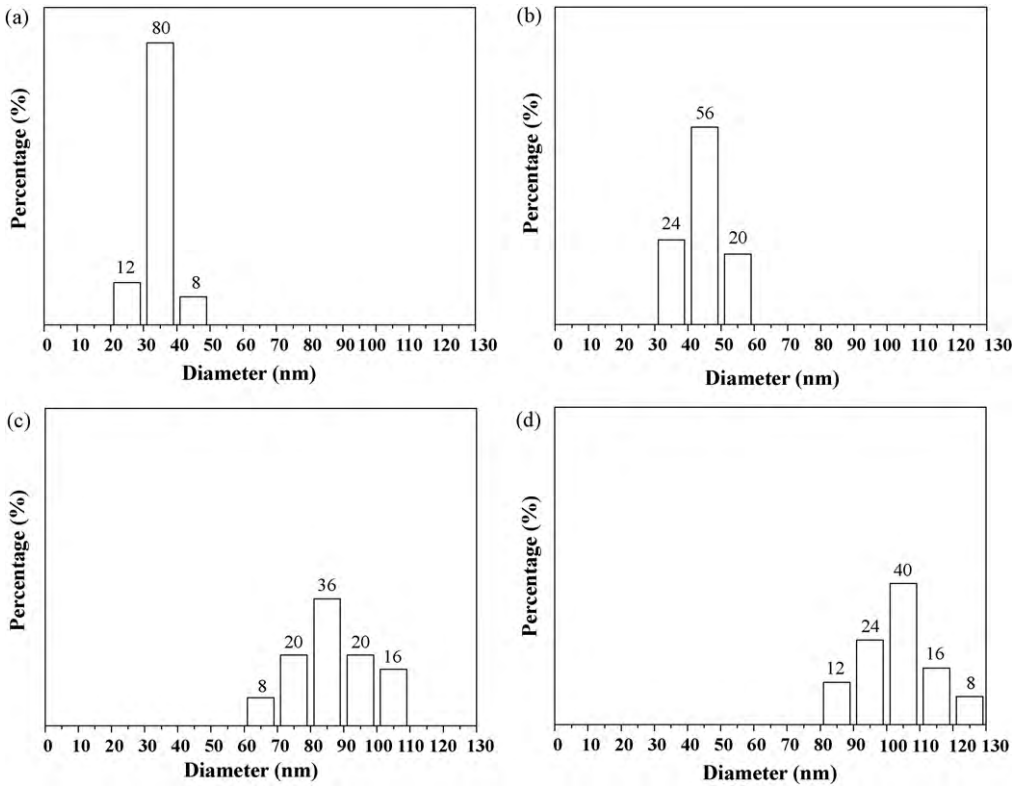

Fig. 2. Diameter distributions of the products by heating the Au-coated TiAlN substrates with Au thicknesses of (a) 3, (b) 5, (c) 9, and (d) 27 nm.

34.6, 44.6, 86.6, and 103.4 nm. It is noteworthy that the diameter of nanowires overall increased with increasing the Au layer thickness. In a previous study, we have revealed that the size and morphology of the underlying Au nanostructures have affected the diameter of the resultant MgO nanowires [26]. Accordingly, we expect that the nanowire diameter could be related to that of the Au nanoparticle on the substrates. The Au nanoparticle is supposed to be the place on which the nanowire sprouts and grows. By heating of the thinner Au layer, we obtain the smaller Au nanoparticles, presumably generating the thinner nanowires. On the other hand, it is difficult to generate the isolated small Au particles by heating the thicker Au layer. In this case, it is surmised that the continuous Au layers or huge Au particles are generated even after the thermal heating and thus the numerous nuclei are co-present on the connected Au surface. Accordingly, as the nuclei grow, they can be easily agglomerated to form thick wires or clusters, rather than thin nanowires.

Several researchers have reported the growth of nanowires by means of direct heating of substrates, with the catalytic metal layer being coated. Yu and co-workers reported the growth of amorphous Si (a-Si) nanowires by the simple heating of Si substrates with the predeposited Ni layer [27]. They found that the growth of a-Si nanowires was controlled by a solid–liquid–solid (SLS) mechanism, in which the only possible Si source came from the Si substrate and Si nanowires grow from the Si_xNi eutectic liquid droplets. Similarly, the growth of SiO_x nanowires on Si was reported using a Pd/Au thin film [28], a Pt thin film [29], and a Co thin film as catalysts [30], in which the Si source was Si substrate. In these cases, the tips of the nanowires are supposed to comprise metal silicide particles, playing a catalytic role. However, in case of SiO_x nanowires, oxygen vapors should be inevitably involved, implying that the associated growth mechanism is a vapor–liquid–solid (VLS) process.

Since no extra Ti source was introduced in the vapor phase of the present study, we suggest that the only possible Ti source should be the TiAlN layer. In the present work, Ti, Au, and Al were the main elements and from the binary Au–Ti and Al–Ti diagram. The

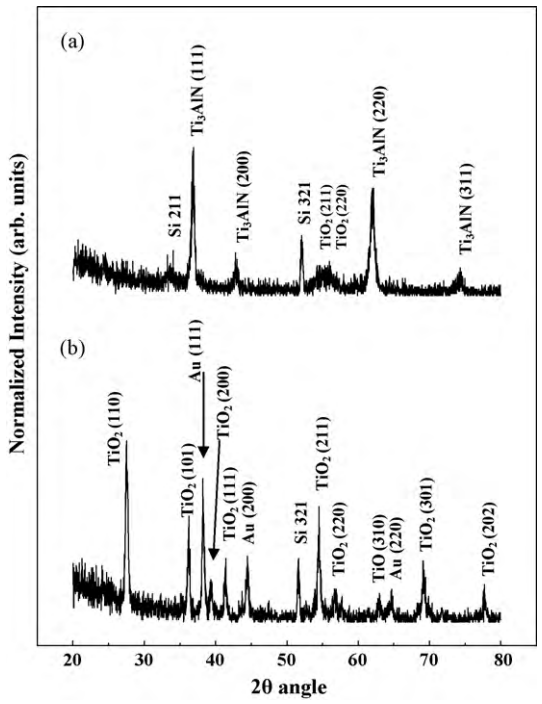

Fig. 3. XRD patterns of the products by heating (a) the uncoated and (b) the Au-coated TiAlN substrates.

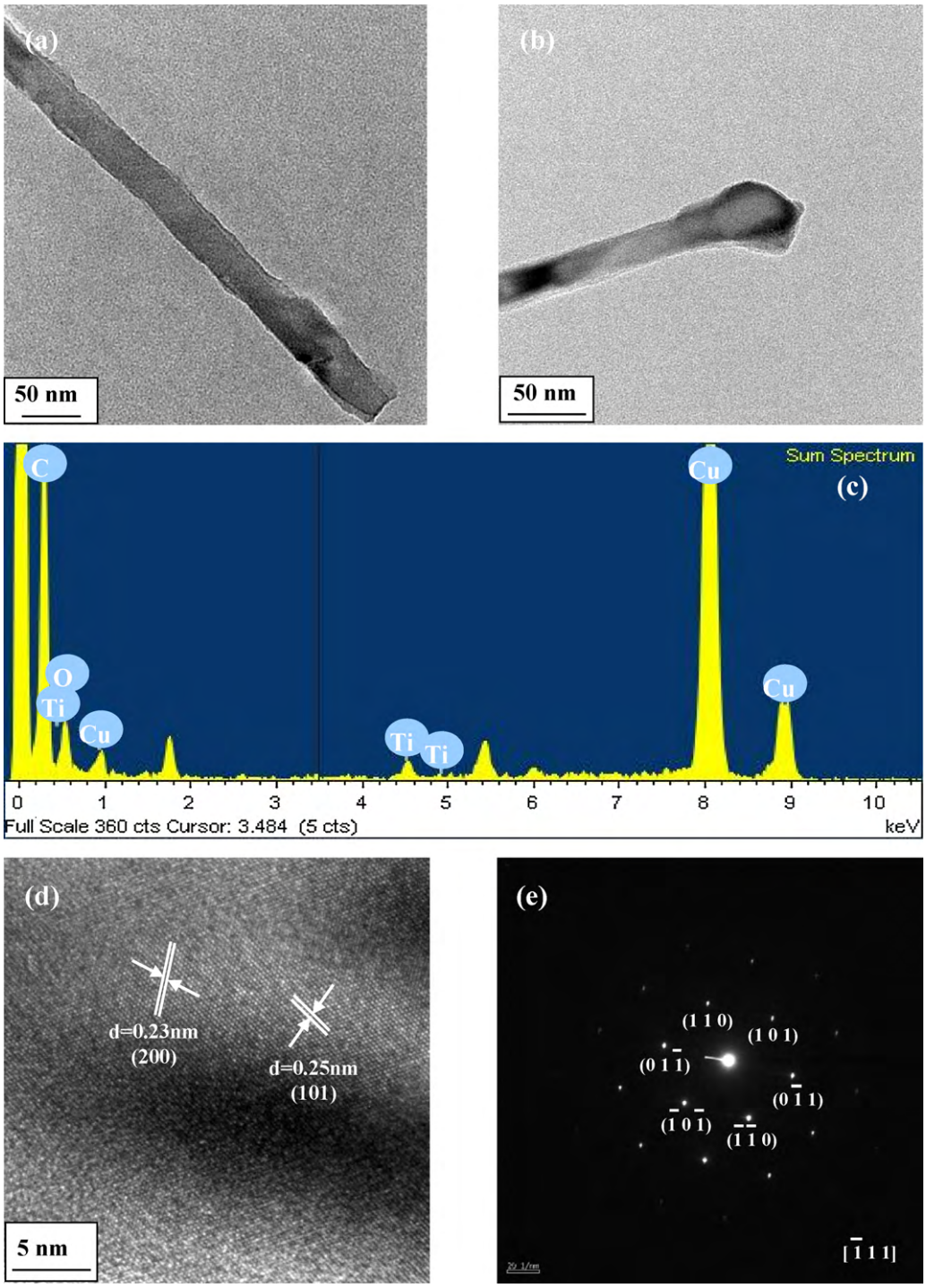

Fig. 4. (a, b) Low-magnification TEM images of typical nanowires. (c) EDX spectrum showing the presence of Ti and O. The Cu signal is from background scattering off the TEM copper grid. (d) Lattice-resolved TEM image and (e) associated SAED pattern.

melting point of the alloy is expected to be lowered by the addition of Au or Al elements, indicating that the Au or Al facilitate the generation of liquid alloy droplets. The most likely source of oxygen may come from the O_2 in the carrier gas [31] and the liquid or solid particles should easily adsorb oxygen. As the droplets or particles become supersaturated, TiO_2 nanowires are formed, possibly by the reaction between Ti and O. TEM investigation revealed that no catalytic particles were observed at the tips of the nanowires, excluding the possibility that the associated mechanism is a tip-growth VLS process. Instead, there may be two possibilities. One is that this type of growth might be the base-growth VLS mechanism. In this type of VLS process, the Au nanoparticle may stay at the bottom of the nanowires during the growth process. Similarly, previous work on the production of CNTs [32] revealed that the growth can be ascribed to the base-growth mechanism, in which the metal catalyst remains situated at the bottom of the

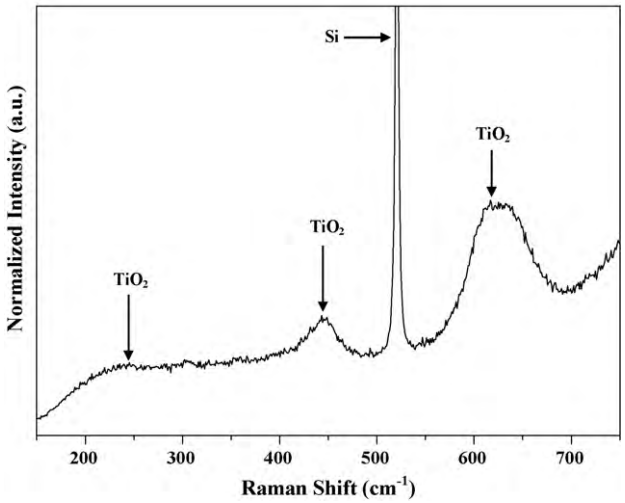

Fig. 5. Raman spectrum of the product grown by heating the Au-coated TiAlN substrate with a Au thickness of 3 nm.

nanostructures. The other possibility may lie in the base-growth vapor–solid–solid (VSS) mechanism, in which the catalytic particles or islands are solid, rather than liquid. Further systematic study is underway in order to reveal the detailed growth mechanism.

Fig. 3a and b shows XRD patterns of the products with uncoated and Au-coated TiAlN substrate, respectively. Fig. 3a reveals that a small fraction of Ti_3AlN phase has been transformed to a TiO_2 phase by thermally heating the bare substrate. The products obtained by heating the Au-coated substrates clearly exhibited a TiO_2 phase, as well as Au phase (Fig. 3b). The TiO_2 tetragonal phase has lattice parameters of $a = 4.593$ Å and $c = 2.959$ Å (JCPDS Card No. 21-1276) with a space group of $P4_2/mnm$, whereas the Au face-centered-cubic phase has a lattice parameter of $a = 4.078$ Å (JCPDS Card No. 04-0784). Since we intended to investigate the properties of TiO_2 nanowires with the smaller dimension, we carried out the TEM study of the TiO_2 nanowires deposited on the substrates with the Au layer thickness of 3 nm. Fig. 4a and b shows low-magnification TEM images, indicating that the tip part of nanowires exhibited a variety of morphology. However, EDX analysis revealed that the nanowire comprised Ti and O elements, regardless of position in the nanowire. Fig. 4c shows a typical EDX spectrum of the tip parts of the nanowires, in which C and Cu peaks were raised from TEM Cu grid coated with amorphous carbon film. No catalytic droplet or nanoparticle was observed at the tips of the nanowires, regardless of the tip morphology. Fig. 4d exhibits the lattice-resolved TEM image of a single nanowire, illustrating that the nanowire is crystalline. The interplanar spacings are approximately 0.23 and 0.25 nm, corresponding to the distance of the neighboring (2 0 0) and (1 0 1) planes in tetragonal TiO_2 structure. Fig. 4e shows an associated selected area electron diffraction (SAED) pattern, which was recorded perpendicular to the nanowire long axis, being indexed for [$\bar{1}$ 1 1] zone axis of crystalline TiO_2. Fig. 5 shows Raman spectrum of the product grown by heating the Au-coated TiAlN substrate with a Au thickness of 3 nm. The sharp peak at 520 cm^{-1} was identified as the TO phonon mode in the silicon (Si) crystal structure [33], presumably from the Si substrates. In addition, the characteristic modes of the rutile TiO_2 phases are located at the wavenumbers of 243, 446, and 613 cm^{-1}, respectively [24,34,35].

Fig. 6a shows the PL spectrum of the products grown by heating the bare TiAlN substrate, whereas Fig. 6b, c, and d shows the PL spectra of the products by heating the Au-coated TiAlN substrate with a Au thickness of 3, 9, and 27 nm, respectively. For detailed analysis, we have deconvoluted the spectrum with Gaussian functions. The PL spectrum shown in Fig. 6a can be deconvoluted into three peaks, which are centered at 3.0, 2.6, and 2.3 eV, respectively. Although XRD spectrum exhibited both Ti_3AlN and TiO_2 phases, to our knowledge, there has been no report on the luminescence from Ti_3AlN phase. It has been known that PL band of TiO_2 located at 3.0 eV is ascribed to self-trapped excitons [21,24]. In particular, Wu et al. postulated that the 3.0-eV peaked band is attributed to self-trapped excitons localized on TiO_6 octahedral [24]. Apart from the self-trapped excitons, oxygen vacancies and surface states are the physical origin of PL spectra of anatase TiO_2 materials [21]. It has been reported that the surface state and oxygen vacancies in TiO_2 nanowires could cause a broad peak at 2.3–3.0 eV bands [24]. In particular, the emission at 2.6 eV [36] and 2.3 eV [37] can be ascribed to the charge-transfer transition from Ti^{3+} to oxygen anion in a TiO_6^{8-} complex associated with oxygen vacancies at the surface. Accordingly, we surmise that the peaks at 2.6 and 2.3 eV are ascribed to the oxygen vacancies at the surface of the TiO_2 nanowires. For Fig. 6b–d, we have deconvoluted the spectra with Gaussian functions, revealing that it can be deconvoluted into four peaks, which are centered at 3.0, 2.6, 2.3, and 1.5 eV, respectively. While the peaks at 3.0, 2.6, and 2.3 eV are similar to those observed in Fig. 6a, the peak at 1.5 eV has been newly observed in Fig. 6b–d. The emission band in the infrared region (at around 1.5 eV) is known to be associated with the formation of Ti^{3+} ions and the related defect states [24]. In the rutile structure, each Ti^{4+} ($3d^0$) ions is surrounded by an octahedron of six O^{2-} ions [38]. Structural defects can be formed by losing an oxygen atom, and the defect states associated with Ti^{3+} ions appear to be introduced. Infrared luminescent transitions associated with Ti^{3+} in rutile structure were previously reported [39].

By comparing Fig. 6b with Fig. 6a, we revealed that all peaks have been significantly intensified by changing into nanowired structures. We surmise that this intensification is ascribed to the increased amounts of products, rather than the changes in morphology. From Fig. 6b and c, we observed that the intensity of visible emissions was decreased with increasing the thickness of the predeposited Au layer. One possibility is that the reduction of intensity is associated with the decreased amounts of products. By simple calculation, we found that the volume of the nanowire films decreased with increasing the Au layer in the range of 3–27 nm. The other possibility is that the visible emission can be enhanced with the nanowire diameter being reduced. Since the average diameter of TiO_2 nanowires increased with increasing the Au layer thickness, we surmise that the surface/volume ratio of the nanowires will decrease with increasing the Au layer thickness. Similarly, Hong et al. reported that TiO_x nanotubes exhibited the enhanced visible emission compared to the TiO_x powders [8], resulting from the more multitudinous existence of surface states in TiO_x nanotubes. On the other hand, Fig. 6b–d indicates that the intensity of 1.5-eV peaked emission slightly increased with increasing the thickness of the predeposited Au layer. Since one possible origin of the 1.5-eV peaked emission is regarded as the defect states in TiO_2, the density (per volume) of which will decrease by increasing the diameter/amounts of nanowires, and thus this mechanism alone cannot explain the observed phenomenon. Accordingly, we suggest that the observation is ascribed to another mechanism; one possibility is that Au layer or nanoparticles mainly located on the substrate contributed to the increase of 1.5-eV peaked emission in the resulting spectra. The literature survey revealed that Au clusters can emit a luminescence spectrum peaked in the range 1.1–1.6 eV [40].

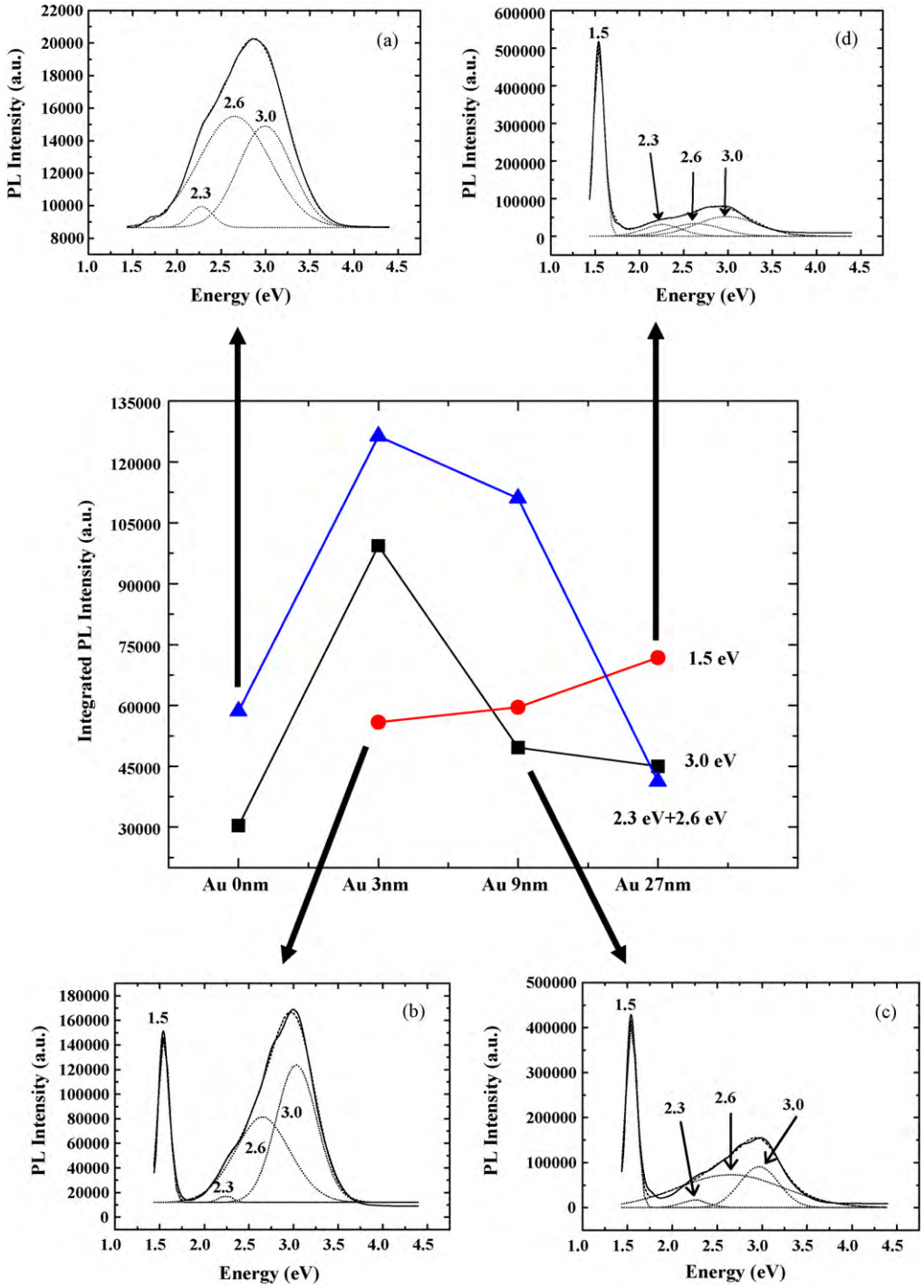

Fig. 6. Integrated PL intensities of 1.5-eV peaked bands, 3.0-eV peaked bands, and the sum of (2.3-peaked and 2.6-peaked) bands, which are deconvoluted from the PL spectra of the products by heating the Au-coated TiAlN substrates with Au thicknesses of (a) 0, (b) 3, (c) 9, and (d) 27 nm.

4. Conclusions

In summary, in fabricating the TiO_2 nanowires via a simple heating of Au-coated TiAlN substrates, we investigated the effect of the thickness of Au layer. The average diameter of produced nanowires increased with increasing the Au layer thickness. XRD, HRTEM image, SAED pattern, and Raman spectrum coincidentally reveal that the obtained nanostructure is categorized into the tetragonal rutile TiO_2 structure. Based on the SEM images on the nanowire morphology, we have speculated on the associated growth mechanism. Since the nanowire morphology is dependent on the Au layer thickness and the nanowire tips do not comprise Au-related particles, we suggest that the associated growth mechanism is a base-growth process. The PL spectra of TiO_2 nanowires produced from the Au-coated substrates were deconvoluted into four peaks, which are centered at 3.0, 2.6, 2.3, and 1.5 eV, respectively. The rel-

ative intensity of visible emission in the range of 2.3–3.0 eV tends to decrease with increasing the predeposited Au layer.

Acknowledgements

This work was supported by a Korea Research Foundation Grant funded by the Korean Government (MOEHRD) (KRF-2007-521-D00216). The main calculations were performed by the supercomputing resources of the Korea Institute of Science and Technology Information (KISTI).

References

[1] K. Huo, X. Zhang, J. Fu, G. Qian, Y. Xin, B. Zhu, H. Ni, P.K. Chu, J. Nanosci. Nanotechnol. 9 (2009) 3341–3346.
[2] K.Y. Cheung, C.T. Yip, A.B. Djurisic, Y.H. Leung, W.K. Chan, Adv. Funct. Mater. 17 (2007) 555–562.
[3] B. O'Regan, M. Gratzel, Nature 353 (1991) 737.
[4] A. Linsebigler, G. Lu, J.T. Yates, Chem. Rev. 95 (1995) 735.
[5] M. Anpo, T. Shima, S. Kodama, Y. Kuybokawa, J. Phys. Chem. 91 (1987) 4305.
[6] A. Fujishima, K. Honda, Nature 238 (1972) 37.
[7] K. Zakrzewska, Thin Solid Films 391 (2001) 229.
[8] J. Hong, J. Cao, J. Sun, H. Li, H. Chen, M. Wang, Chem. Phys. Lett. 380 (2003) 366.
[9] Y.N. Xia, P.D. Yang, Adv. Mater. 15 (2003) 351.
[10] A. Hagfeldt, M. Grätzel, Chem. Rev. 95 (1995) 49.
[11] M. Adachi, I. Okada, S. Ngamsinlapasathian, Y. Murata, S. Yoshikawa, Electrochemistry 70 (2002) 449.
[12] S.L. Zhang, J.F. Zhou, Z.J. Zhang, Z.L. Du, A.V. Vorontsov, Z.S. Jin, Chin. Sci. Bull. 45 (2000) 1533.
[13] G. Crotty, T. Daud, R. Kachare, J. Appl. Phys. 61 (1987) 3077.
[14] B.H. Lee, Y. Jeon, K. Zawadzki, W.J. Qi, J. Lee, Appl. Phys. Lett. 74 (1999) 3143.
[15] G. Banfi, V. Degiorgo, D. Ricard, Adv. Phys. 47 (1998) 447.
[16] W.I. Milne, K.B.K. Teo, G.A.J. Amaratunga, P. Legagneux, L. Gangloff, J.-P. Schnell, V. Semet, V. Thien Binh, O. Groening, J. Mater. Chem. 2004 (2004) 933.
[17] S.K. Pradhan, P.J. Reucroft, F. Yang, A. Dozier, J. Cryst. Growth 256 (2003) 83.
[18] J.-J. Wu, C.-C. Yu, J. Phys. Chem. B 108 (2004) 3378.
[19] G.H. Du, Q. Chen, R.C. Che, Z.Y. Yuan, L.-M. Peng, Appl. Phys. Lett. 79 (2001) 3702.
[20] P. Hoyer, Langmuir 12 (1996) 1411.
[21] Y. Lei, L.D. Zhang, G.W. Meng, G.H. Li, X.Y. Zhang, C.H. Liang, W. Chen, S.X. Wang, Appl. Phys. Lett. 78 (2001) 1125.
[22] X.Y. Zhang, L.D. Zhang, W. Chen, G.W. Meng, M.J. Zheng, L.X. Zhao, Chem. Mater. 13 (2001) 2511.
[23] C.-C. Wang, C.-Y. Yu, C.-C. Kei, C.-T. Lee, T.-P. Perng, Nanotechnology 20 (2009) 285601.
[24] J.-M. Wu, H.C. Shih, W.-T. Wu, Y.-K. Tseng, I.-C. Chen, J. Cryst. Growth 281 (2005) 384.
[25] H.W. Kim, N.H. Kim, J.H. Myung, S.H. Shim, Phys. Status Solidi A 202 (2005) 1758.
[26] H.W. Kim, S.H. Shim, Chem. Phys. Lett. 422 (2006) 165.
[27] H.F. Yan, Y.J. Xing, Q.L. Hang, D.P. Yu, Y.P. Wang, J. Xu, Z.H. Xi, S.Q. Feng, Chem. Phys. Lett. 323 (2000) 224.
[28] J.L. Elechiguerra, J.A. Manriquez, M.J. Yacaman, Appl. Phys. A 79 (2004) 461.
[29] P.K. Sekhar, S.N. Sambandam, D.K. Sood, S. Bhansali, Nanotechnology 17 (2006) 4606.
[30] H.W. Kim, S.H. Shim, Appl. Surf. Sci. 253 (2007) 3664.
[31] H.W. Kim, S.H. Shim, J.W. Lee, Physica E 37 (2007) 163.
[32] S. Fan, M.G. Chapline, N.R. Franklin, T.W. Tombler, A.M. Cassell, H. Dai, Science 283 (1999) 512.
[33] M. Hirasawa, T. Orii, T. Seto, Appl. Phys. Lett. 88 (2006) 093119.
[34] V.A. Skryshevskyy, Th. Dittrich, J. Rappich, Phys. Status Solidi A 201 (2004) 157.
[35] H. Chang, P.J. Huang, J. Raman Spectrosc. 29 (1998) 97.
[36] J. Liu, J. Li, A. Sedhain, J. Lin, H. Jiang, J. Phys. Chem. C 112 (2008) 17127.
[37] J.C. Yu, J. Yu, W. Ho, Z. Jiang, L. Zhang, Chem. Mater. 14 (2002) 3808.
[38] R. Sanjines, H. Tang, H. Berger, F. Gozzo, G. Magaritondo, F. Levy, J. Appl. Phys. 75 (1994) 2945.
[39] A.K. Ghosh, F.G. Wakim, R.R. Addiss Jr., Phys. Rev. 184 (1969) 979.
[40] L. Prodi, G. Battistini, L. S. Dolci, M. Montalti, N. Zaccheroni, Springer Series in Optical Sciences vol. 133 (2007) 99, Springer, Berlin/Heidelberg, Germany.